Advancements in Transparent Conducting Oxides: Amorphous IO & ZITO

Brett Freese, Timothy Holmes, Manuel Osorio, Miko Stulajter, and Gabriela González Avilés

Department of Physics

DePaul University

Abstract In this research project, we set out to discover why the compounds indium oxide (IO) and zinc-indium-tin-oxide (ZITO) are better semiconductors in their amorphous state, just before they become crystalline. A series of IO and ZITO thin films ranging from fully amorphous to fully crystalline were prepared. We analyzed their x-ray pair distribution function data collected at Argonne National Laboratory. We evaluated the films' lateral and depth uniformity by analyzing different sections (in plane, out of plane and average) of the data that were measured at different penetration depths. A variety of software packages were used, including GSAS II, PDFgetX3, and MATLAB. For both IO and ZITO, we found that the in-plane and out-of-plane atomic structures differed suggesting that the films are not laterally homogeneous. Shorter bond lengths correlated with high electron mobility. These results will be compared with molecular dynamic simulations to better understand which local atomic structure produces enhanced electrical properties.

Motivation

Transparent Conducting Oxides (TCOs) are semiconductors that have high electrical conductivity and are transparent in the visible region. TCO crystalline electrodes are used in the electronics industry in flat-panels, solar cells, and energy-efficient windows. Some amorphous TCOs benefit from having increased electrical properties as well as improved mechanical properties. Because amorphous TCOs are not rigid, they can be deposited on plastic substrates, which can flex without breaking, further expanding their applications.

TCO electrodes in current commercial applications are indium-oxide (IO) based. This research project focused on studying one series of undoped IO and two series (thin and thick) of zinc-indium-tin oxide (ZITO) films. ZITO is obtained by doping indium oxide with zinc and tin, and it can be prepared in its amorphous state at higher temperatures compared to undoped IO.

The samples were grown at different temperatures by pulsed laser deposition at Northwestern University. Below are the spectra graphs for the ZITO thin samples, which ranged from 350-450 nm in thickness. Alongside it (to the right) are the graphs of hall mobility as a function of the deposition temperature. For the spectra graph (left), sharp features indicate crystallinity in the structure. The graph shows that below 150 ℃, the samples were fully amorphous. The degree of crystallinity increased with temperature.

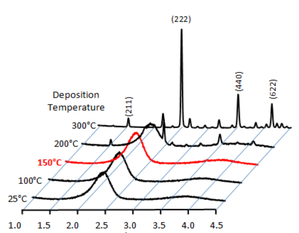

Figure 1 Below 150℃, the films are amorphous. At 200℃, the sample becomes semi-crystalline, and at 300℃ the material is fully crystalline.

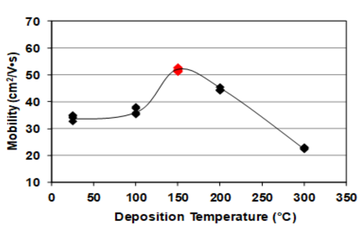

Figure 2: The highest-temperature amorphous ZITO sample shows the best electron mobility.

The graph on the right shows how the electron mobility changes as a function of deposition temperature. The sample deposited at 150 ℃, which is the last amorphous sample in the series, possesses the highest electron mobility. Similar behavior is observed for ZITO thick (~1000 nm) films and for undoped IO films (~400 nm thick). This tells not all amorphous samples are the same, and that right before any crystallinity is observed, mobility is maximized in both IO and ZITO.

X-Ray Scattering Experiments and Analysis

The x-ray pair-distribution function (PDF) measurements were conducted at the Advanced Photon Source at Argonne National Laboratory. High energy (70 keV) x-ray beams were used to scatter from the samples at very shallow incident angles. The x-ray patterns were recorded on four different two-dimensional General Electric (GE) detectors, as shown below. The regions that measure the horizontal sections of the images are called "in plane." The "out-of-plane section was orthogonal to the in-plane, and probed the vertical section of the images. The two sections are faintly visible (outlined in red and blue) in the image on the right. The "average" section encompassed the entire upper semicircle.

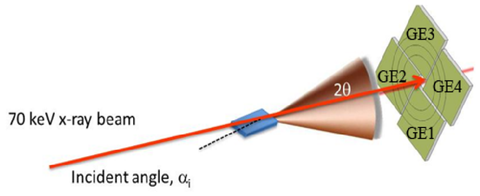

Figure 3: Schematic of the experimental setup, showing the sample and the arrangement of the four-panel array of 2D detectors.

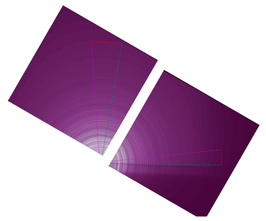

Figure 4: 2-D detectors: GE3 measures the out-of-plane and GE4 measures the in plane regions.

Five different incident angles (α_i) were used: 0.04°, 0.05° (critical angle), 0.06°, 0.10°, and 0.15° to study the depth uniformity in ZITO films. For IO samples, two incident angles were used: at the critical angle, and at two times the critical angle. The lower angle measures only the surface of the film, while the bigger angle probes the whole thickness of the film.

The analysis of the data included integrating the 2D images into 1D data files with GSAS II [1]. PDFGEXT3 [2] was used to Fourier transform the data and subtract the substrate signal. Custom MATLAB [3] scripts were then used to fit and obtain the peak area (proportional to the coordination number), peak position (bond length), and peak width (proportional to the disorder) for the first coordination shells (metal-O, and metal-metal pairs).

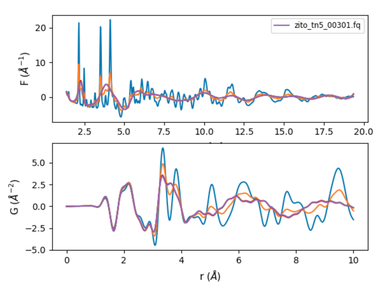

Figure 5: Top panel: data after radial integration for the ZITO thick series. Each color represents one sample grown at a different deposition temperature. Bottom panel: pair distribution function (PDF) signals after Fourier transformation and substrate subtraction. Information about the atomic pairs is extracted from the PDF data.

The PDF data (lower panel) for all samples were normalized so that the In-O shell amplitudes match after subtraction of the silica substrate. The peak ~ 2.2 Å corresponds to the In-O shortest pair (1st shell). The peaks ~ 3.3 and 3.8 Å correspond to the metal-metal (2nd, and 3rd) pairs. The amorphous samples only show short-range ordering, as the sharp features stop ~5 Å; while the crystalline samples exhibit atomic ordering for a longer distance.

[1] Toby B. H. and Von Dreele R. B., "GSAS-II: the genesis of a modern open-source all purpose crystallography software package". *J. Appl. Cryst.* 46(2), 544-549, 2013.

[2] Juhas P., Davis T., Farrow C.L., and Billinge S.J.L. "PDFgetX3: a rapid and highly automatable program for processing powder diffraction data into total scattering pair distribution functions". *App. Cryst.*, 46, 560-566, 2013.

[3] MATLAB Release 2016a, The MathWorks, Inc., Natick, Massachusetts, USA.

IO and ZITO Results

- Tin and zinc dopants increase the amorphous range in IO by 150 ℃.
- All samples have lateral as well as depth gradients.
  - The major differences occur in the in plane vs. out-of-plane directions.
  - The data collected as a function of incident angle show that the atoms at the surface are more disordered compared to the film interior.
- Amorphous TCO films consistently have lower coordination numbers than crystalline samples.
- For all three TCO series, the shortest bond lengths for the first three coordination shells correspond to the amorphous samples with the highest mobility. These samples are always deposited at the highest temperatures (T= 150 ℃ for ZITO and T = 0℃ for IO) when the samples are still amorphous, just before they crystallize.
- For amorphous samples, shell 3 splits into two distinct shells (3 and 4).

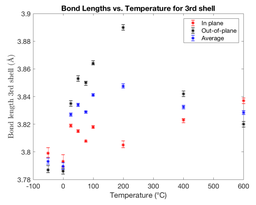

Figure 6: Bond length of the 3rd (metal-metal) shell in IO as a function of deposition temperature. The two amorphous samples (below 0°C) have lower bond lengths. The semi-crystalline samples are textured and have a high lateral anisotropy.

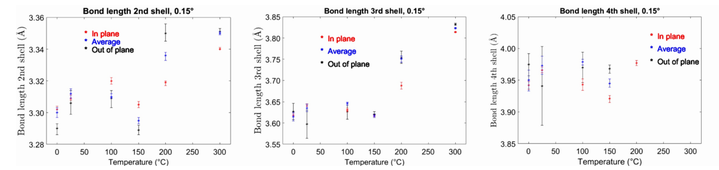

Figure 7: Bond length of the second, third, and fourth (metal-metal) shells in ZITO as a function of deposition temperature. The sample prepared at 150 °C has the shortest bond length for the 2nd shell. The third and fourth shells merge into a single shell when the samples crystallize.

- In IO, peak width decreases as the samples become more crystalline. Furthermore, the in-plane and out-of-plane peak widths merge. Both observations indicate a higher degree of ordering at very high temperatures. When the atoms have more energy, they arrange themselves for longer distances, yielding fully crystalline samples.

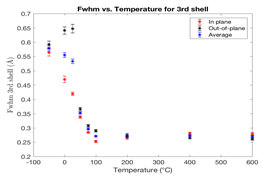

Figure 8: The full width at half maximum (FWHM) of the third shell in IO as a function of deposition temperature.

Conclusions and Future Work

The electrical mobility of indium-based TCOs shows similar trends: the best properties are obtained in amorphous samples just before crystallization. This enhanced mobility is correlated to the atomic local ordering in the samples, when the bond lengths are the shortest. Lateral and depth gradients in the films are present. Doping IO with zinc and tin increases the amorphous range of the films, well above room temperature. All the structural results from this study will be compared to molecular dynamic simulations performed by theoreticians. Further experiments with oxynitrides and oxyfluorides will be conducted to expand the performance of amorphous semiconductors.

Acknowledgements: This project was funded by the NSF-MRSEC grant number DMR-1121262. The x-ray experiments were conducted at Sector 1 of the APS, which is funded by the Office of Science, Office of Basic Energy Sciences in the U.S. Department of Energy. Bruce D. Buchholz prepared the samples and measured their electrical properties at Northwestern University.